Eur. Phys. J. C (2018) 78:451
https://doi.org/10.1140/epjc/s10052-018-5918-6

THE EUROPEAN PHYSICAL JOURNAL C

Letter

Long-distance effects in $B \to K^* \ell\ell$ from analyticity

Christoph Bobeth[1,2], **Marcin Chrzaszcz**[3,4,a], **Danny van Dyk**[3], **Javier Virto**[1,5]

[1] Physik Department, TU München, James-Franck-Straße 1, 85748 Garching, Germany
[2] Excellence Cluster Universe, Technische Universität München, Boltzmannstr. 2, 85748 Garching, Germany
[3] Physik-Institut, Universität Zürich, Winterthurer Strasse 190, 8057 Zürich, Switzerland
[4] H.Niewodniczanski, Institute of Nuclear Physics Polish Academy of Sciences, ul. Radzikowskiego 152, 31-342 Krakow, Poland
[5] Center for Theoretical Physics, Massachusetts Institute of Technology, Cambridge, MA 02139, USA

Received: 3 March 2018 / Accepted: 19 May 2018 / Published online: 5 June 2018

Abstract We discuss a novel approach to systematically determine the dominant long-distance contribution to $B \to K^* \ell\ell$ decays in the kinematic region where the dilepton invariant mass is below the open charm threshold. This approach provides the most consistent and reliable determination to date and can be used to compute Standard Model predictions for all observables of interest, including the kinematic region where the dilepton invariant mass lies between the J/ψ and the $\psi(2S)$ resonances. We illustrate the power of our results by performing a New Physics fit to the Wilson coefficient C_9. This approach is systematically improvable from theoretical and experimental sides, and applies to other decay modes of the type $B \to V\ell\ell$, $B \to P\ell\ell$ and $B \to V\gamma$.

1 Introduction

$B \to K^* \ell\ell$ decays are sensitive to modified short-distance physics from sources beyond the Standard Model (SM), and a great deal of experimental and theoretical work has been devoted to extract short-distance information from them. However, long-distance physics within the SM also contributes significantly to the decay, and its effects are very difficult to assess reliably from first principles. On the other hand, tighter experimental constraints from increasingly precise measurements of $b \to s$ processes have significantly limited the size of allowed New Physics (NP) effects in $B \to K^* \ell\ell$, which are now comparable to current SM uncertainties. Thus, our inability to reliably constrain these long-distance contributions to acceptable levels stands in the way of obtaining unambiguous information on physics beyond the SM.

[a] e-mail: mchrzasz@cern.ch

The $B \to K^* \ell\ell$ decay is conveniently described by the K^* transversity amplitudes ($\lambda = \perp, \parallel, 0$)

$$\mathcal{A}_\lambda^{L,R} = \mathcal{N}_\lambda \left\{ (C_9 \mp C_{10}) \mathcal{F}_\lambda(q^2) + \frac{2 m_b M_B}{q^2} \left[C_7 \mathcal{F}_\lambda^T(q^2) - 16\pi^2 \frac{M_B}{m_b} \mathcal{H}_\lambda(q^2) \right] \right\} \quad (1)$$

where $C_{7,9,10}$ are short-distance Wilson coefficients, and $\mathcal{N}_\lambda$ are normalization factors. The non-trivial matter from the theory point of view is the determination of the "local" and "non-local" long-distance effects encoded in the functions $\mathcal{F}_\lambda^{(T)}(q^2)$ and $\mathcal{H}_\lambda(q^2)$, respectively, which depend on the dilepton invariant mass squared q^2.

The functions $\mathcal{F}_\lambda^{(T)}(q^2)$ are form factors, which can be calculated by means of Light-Cone Sum Rules (LCSRs) at low q^2 ($\lesssim 10$ GeV^2) [1,2], or by numerical simulations (Lattice QCD) at large q^2 ($\gtrsim 15$ GeV^2) [3,4]. Both methods agree reasonably well when extrapolated [5,6], and there are good prospects for improvement [7–11]. The form factors are not the focus of this work.

Here we focus on the functions $\mathcal{H}_\lambda(q^2)$, which are related to the contribution from 4-quark and chromomagnetic operators in the Weak Effective Hamiltonian, and emerge from the "non-local" matrix element

$$\eta_\alpha^* \mathcal{H}^{\alpha\mu} \equiv i \int d^4x \, e^{iq\cdot x} \langle \bar{K}^*(k,\eta) | \mathcal{K}^\mu(x,0) | \bar{B}(p) \rangle \,, \quad (2)$$

where $p = q + k$, η is the polarization vector of the K^*, and $\mathcal{K}(x, y)$ is a bi-local operator. The most relevant contribution to this matrix element in the SM arises from the current-current operators $\mathcal{O}_{1,2}$, since they come with large Wilson coefficients. In this letter we consider only this contribution – the so-called "charm-loop effect" – for which the object $\mathcal{K}^\mu(x, y)$ is given by:

$$\mathcal{K}^\mu(x,y) = T\left\{j^\mu_{\rm em}(x), C_1\mathcal{O}_1(y) + C_2\mathcal{O}_2(y)\right\} \tag{3}$$

with $j^\mu_{\rm em}(x) = \sum_q Q_q\, \bar q(x)\gamma^\mu q(x)$ the electromagnetic current. The scalar functions $\mathcal{H}_\lambda(q^2)$ are given by the Lorentz decomposition:

$$\mathcal{H}^{\alpha\mu}(q,k) = M_B^2\left[S_\perp^{\alpha\mu}\,\mathcal{H}_\perp - S_\parallel^{\alpha\mu}\,\mathcal{H}_\parallel - S_0^{\alpha\mu}\,\mathcal{H}_0\right] \tag{4}$$

where $S_\lambda^{\alpha\mu}$ are a set of structures given in the appendix.

In the heavy b-quark limit and for very small q^2, the functions $\mathcal{H}_\lambda(q^2)$ factorize into non-perturbative form factors and light-cone distribution amplitudes, up to perturbatively calculable "hard" functions [12]. However this perturbative expansion breaks down when q^2 approaches $4m_c^2$, leading to questionable predictions for $q^2 \gtrsim 6\,\text{GeV}^2$. The integral in Eq. (2) is in fact dominated by the region $x^2 \lesssim (2m_c - \sqrt{q^2})^{-2}$ [13], so for $q^2 \ll 4m_c^2$ one may expand the operator $\mathcal{K}^\mu(x,0)$ around $x^2 = 0$ (a light-cone operator-product expansion, or LCOPE). This leads to an expansion of Eq. (2) in powers of $(2m_c - \sqrt{q^2})^{-1}$, with matrix elements of operators that are non-local only along the light cone. This theory framework has been worked out up to NLO in α_s [12,14] and including subleading terms in the LCOPE [13], and can be safely applied for $q^2 \ll 4m_c^2$ (preferably at $q^2 < 0$). However, reliable predictions for larger values of q^2 remain a challenge.

In this letter we consider a consistent, model-independent and systematically-improvable approach to determine the dominant long-distance contributions $\mathcal{H}_\lambda(q^2)$ to $B \to K^*\ell\ell$ in the region $q^2 \lesssim 14\,\text{GeV}^2$. It provides genuine SM predictions even in the presence of NP in semileptonic operators. In addition, this approach provides access to the inter-resonance region $10\,\text{GeV}^2 \lesssim q^2 \lesssim 13\,\text{GeV}^2$. The idea is the following: We determine the analytic properties of the functions $\mathcal{H}_\lambda(q^2)$ in the complex plane, by considering their dominant singularities. We then use this information to write down a general and model-independent parametrization. Two pieces of information are used to constrain the parametrized functions: data on $B \to K^* J/\psi$ and $B \to K^*\psi(2S)$, which is independent of NP in semileptonic operators; and theory at $q^2 < 0$, where it is reliable. This method, which builds upon Refs. [13,15], gives the most reliable and consistent *a-priori* determination of the functions $\mathcal{H}_\lambda(q^2)$ to date. We use these results to compute SM predictions (assuming no NP in $\mathcal{O}_{1,2}$), and to perform a NP fit to C_9. All our numerical computations are performed with the help of EOS [16], which has been modified for this purpose [17].

2 Analytic structure and parametrization

It is a standard assumption in quantum field theory that the only analytic singularities of a correlation function – as a complex function of all its complexified kinematic invariants – are those required by unitarity [18]. This principle of "maximal analyticity" can sometimes be derived from causality, and it is therefore well founded [19]. Unitarity, in turn, relates analytic singularities with on-shell intermediate states: poles for one-particle states, and branch cuts for multi-particle states. Thus, the analytic structure of a correlation function can be learned by analysing its on-shell cuts.

In the case at hand, inspection of the correlation function (2) reveals the following analytic properties of the scalar functions $\mathcal{H}_\lambda(q^2)$:

► On-shell cuts in the variable q^2 include: two poles at $q^2 = M^2_{J/\psi} \simeq 9\,\text{GeV}^2$ and $q^2 = M^2_{\psi(2S)} \simeq 14\,\text{GeV}^2$ corresponding to one-particle intermediate states through $B \to K^*\psi_n(\to \ell^+\ell^-)$, with $\psi_1 = J/\psi$ and $\psi_2 = \psi(2S)$; a branch cut starting at $q^2 = t_+ \equiv 4M_D^2$ corresponding to two-particle intermediate states through $B \to K^*[\bar D D](\to \ell^+\ell^-)$, plus other "$c\bar c$" cuts with higher thresholds; and "light-hadron" branch cuts starting at $q^2 \simeq 0$ from intermediate states such as $B \to K^*[3\pi](\to \ell^+\ell^-)$, which include finite-width effects of J/ψ and $\psi(2S)$. The effects of these "light-hadron" cuts are OZI suppressed [20–22]. Given the limited precision of current data, we will neglect these OZI suppressed contributions, keeping in mind that this is a pending assumption that should be tested in view of future experimental prospects. These presumably small effects have never been considered in previous analyses before.

► On-shell cuts in the variable $(q+k)^2$ (the "forward" or "decay" channel) include branch cuts from intermediate states such as $B \to \bar D D_s \to K^*\ell^+\ell^-$. The physical point $(q+k)^2 = M_B^2$ lies on these cuts, which implies that the functions $\mathcal{H}_\lambda(q^2)$ are complex-valued for all values of q^2. But this imaginary part is not associated with any singularity in the variable q^2. Thus, one can write $\mathcal{H}_\lambda(q^2) = \mathcal{H}_\lambda^{(\rm re)}(q^2) + i\,\mathcal{H}_\lambda^{(\rm im)}(q^2)$, with $\mathcal{H}_\lambda^{(\rm re,im)}(q^2)$ satisfying the analytic properties of the previous point as functions of q^2, and obeying the same dispersion relation.

These properties can be exploited to write down a general parametrization for the correlator consistent with unitarity. A convenient way to do so is to re-express the functions $\mathcal{H}_\lambda(q^2)$ in terms of the "conformal" variable z:

$$z(q^2) \equiv \frac{\sqrt{t_+ - q^2} - \sqrt{t_+ - t_0}}{\sqrt{t_+ - q^2} + \sqrt{t_+ - t_0}}, \tag{5}$$

where $t_+ = 4M_D^2$ and $t_0 = t_+ - \sqrt{t_+(t_+ - M^2_{\psi(2S)})}$. This transformation maps the $c\bar c$ branch cut in the q^2 plane to the unit circumference $|z| = 1$, and the entire first Riemann sheet in the q^2 plane to the interior of the unit circle $|z| < 1$. Our choice for t_0 implies that within the relevant interval $-7\,\text{GeV}^2 \le q^2 \le M^2_{\psi(2S)}$, $|z| < 0.52$.

The approach now resembles and is inspired by the z-parametrization used for the form factors [23,24]. The functions $\mathcal{H}_\lambda(z) \equiv \mathcal{H}_\lambda(q^2(z))$ are meromorphic in $|z| < 1$, with two simple poles at $z_{J/\psi} \equiv z(M^2_{J/\psi}) \simeq 0.18$ and $z_{\psi(2S)} \equiv z(M^2_{\psi(2S)}) \simeq -0.44$. Therefore, multiplying by the corresponding zeroes will give an analytic function in $|z| < 1$ that can be Taylor-expanded around $z = 0$. This expansion should converge reasonably well in the region of interest, where $|z| < 0.52$. This is the basis of our proposed parametrization.

In order to assure that the leading terms in the expansion will capture most of the features of the function (thus improving convergence), we use two more pieces of information: First, the correlator inherits all the singularities of the form factor (*e.g.* the $M_{B_s^*}$ pole), and the leading OPE contribution to the correlator is indeed proportional to the form factor. Therefore it is better to parametrize the ratios $\mathcal{H}_\lambda(q^2)/\mathcal{F}_\lambda(q^2)$ instead. Second, the poles should not modify the asymptotic behaviour. This is achieved by introducing appropriate "Blaschke factors" [23]. All in all, we propose the following parametrization:

$$\mathcal{H}_\lambda(z) = \frac{1 - z\, z^*_{J/\psi}}{z - z_{J/\psi}} \frac{1 - z\, z^*_{\psi(2S)}}{z - z_{\psi(2S)}} \hat{\mathcal{H}}_\lambda(z) \,, \tag{6}$$

with

$$\hat{\mathcal{H}}_\lambda(z) = \Big[\sum_{k=0}^{K} \alpha_k^{(\lambda)} z^k \Big] \mathcal{F}_\lambda(z) \,, \tag{7}$$

where $\alpha_k^{(\lambda)}$ are complex coefficients, and the expansion is truncated after the term z^K. This truncation unavoidably introduces some model dependence. The maximum value that can be chosen for K will depend on the available set of experimental measurements and theory inputs.

3 Experimental constraints

According to the LSZ reduction formula [25], the amplitudes for the decays $B \to K^* \psi_n$ (with $\psi_1 = J/\psi$ and $\psi_2 = \psi(2S)$) are defined by the residues of the functions $\mathcal{H}_\lambda(q^2)$ on the ψ_n poles:

$$\mathcal{H}_\lambda(q^2 \to M^2_{\psi_n}) \sim \frac{M_{\psi_n} f^*_{\psi_n} \mathcal{A}_\lambda^{\psi_n}}{M_B^2 (q^2 - M^2_{\psi_n})} + \cdots \,, \tag{8}$$

where the dots represent regular terms. Here $\langle 0 | j^\mu_{\rm em} | \psi_n(q, \varepsilon) \rangle = M_{\psi_n} f^*_{\psi_n} \varepsilon^\mu$, and $\mathcal{A}_\lambda^{\psi_n}$ are the $B \to K^* \psi_n$ transversity amplitudes. The most precise constraints on these amplitudes can be obtained from Babar [26,27], Belle [28–30] and LHCb [31].

We use the data to produce two sets of five pseudo-observables (three magnitudes and two relative phases on each resonance):

$$|r_\perp^{\psi_n}|,\ |r_\parallel^{\psi_n}|,\ |r_0^{\psi_n}|,\ \arg\{r_\perp^{\psi_n} r_0^{\psi_n *}\},\ \arg\{r_\parallel^{\psi_n} r_0^{\psi_n *}\}, \tag{9}$$

where

$$r_\lambda^{\psi_n} \equiv \operatorname*{Res}_{q^2 \to M^2_{\psi_n}} \frac{\mathcal{H}_\lambda(q^2)}{\mathcal{F}_\lambda(q^2)} \sim \frac{M_{\psi_n} f^*_{\psi_n} \mathcal{A}_\lambda^{\psi_n}}{M_B^2\, \mathcal{F}_\lambda(M^2_{\psi_n})} \,. \tag{10}$$

The numerical values for these pseudo-observables are obtained from the posterior-predictive distributions of a Bayesian fit. The inputs for this fit and the results are provided for completeness in the appendix. These pseudo-observables will act as constraints on the parameters of the correlators at $z = 0.18$ and $z = -0.44$.

4 Theory constraints

At $q^2 < 0$ the functions $\mathcal{H}_\lambda$ can be calculated with the current approaches for the large recoil region. We use QCD-factorization at next-to-leading order in α_s, including the form factor terms and hard-spectator contributions [12,32]. In addition, we include[1] the soft-gluon correction calculated via a LCSR in Ref. [13]. For the form factors we use the results from the LCSR with B-meson distribution amplitudes [2], in order to have a mutually consistent description of form factors and non-local contributions and benefit from theoretical correlations among both. In this way we compute the ratios $\mathcal{H}_\lambda(q^2)/\mathcal{F}_\lambda(q^2)$ at the points $q^2 = \{-7, -5, -3, -1\}\,\text{GeV}^2$. These ratios are used as pseudo-observables to constrain the parameters in Eq. (6) at $z = \{0.52, 0.50, 0.48, 0.46\}$. Further details and results are presented for completeness in the appendix. We emphasize that no theory is used at $q^2 \geq 0$ at all.

5 SM predictions

We now perform a fit of Eq. (6) to the combined experimental and theoretical constraints described above in Sects. 3 and 4. We find that Eq. (6) with $K = 2$ provides an excellent fit to all inputs, with a p-value of 0.91. All 1D-marginalised posteriors are reasonably symmetric around their modes. The result of this fit is a set of correlated values for the complex parameters $\alpha_k^{(\lambda)}$, which are summarized in Table 1. These values lead to a determination of the non-local correlator in Eq. (2) that is consistent with the $B \to K^* \psi_n$ measurements,

[1] We thank Yuming Wang for providing us with the results for $B \to K^* \gamma^*$ in digital form.

Table 1 Mean values and standard deviations (in units of 10^{-4}) of the prior PDF for the parameters $\alpha_k^{(\lambda)}$

k	0	1	2
$\mathrm{Re}[\alpha_k^{(\perp)}]$	-0.06 ± 0.21	-6.77 ± 0.27	18.96 ± 0.59
$\mathrm{Re}[\alpha_k^{(\parallel)}]$	-0.35 ± 0.62	-3.13 ± 0.41	12.20 ± 1.34
$\mathrm{Re}[\alpha_k^{(0)}]$	0.05 ± 1.52	17.26 ± 1.64	–
$\mathrm{Im}[\alpha_k^{(\perp)}]$	-0.21 ± 2.25	1.17 ± 3.58	-0.08 ± 2.24
$\mathrm{Im}[\alpha_k^{(\parallel)}]$	-0.04 ± 3.67	-2.14 ± 2.46	6.03 ± 2.50
$\mathrm{Im}[\alpha_k^{(0)}]$	-0.05 ± 4.99	4.29 ± 3.14	–

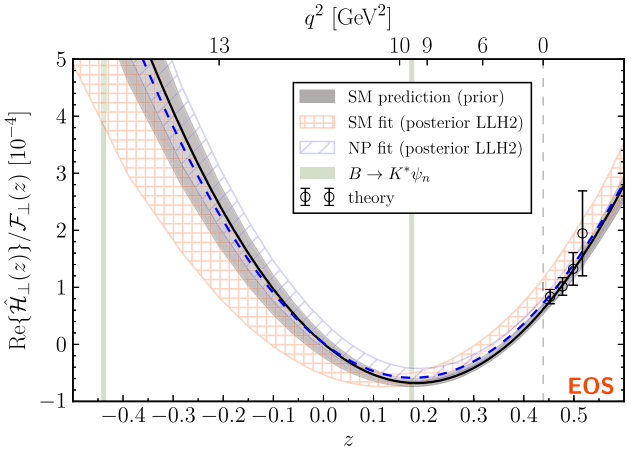

Fig. 1 Results of the prior and posterior fits for the ratio $\mathrm{Re}[\hat{\mathcal{H}}_\perp(z)]/\mathcal{F}_\perp(z)$. See the text for details

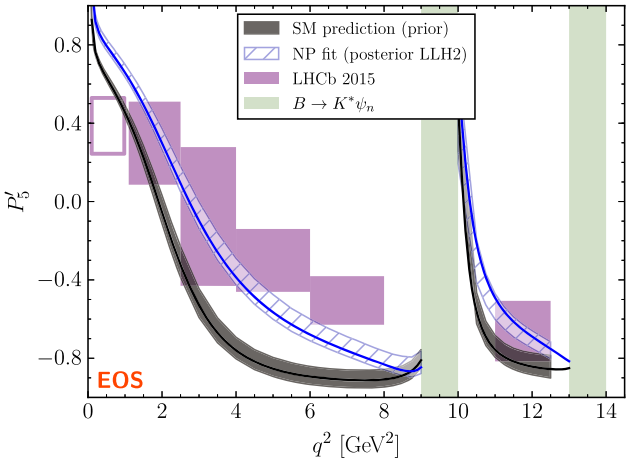

Fig. 2 Prior and posterior predictions for P_5' within the SM and the NP C_9 benchmark, compared to LHCb data

the theory calculations at negative q^2, and it is independent of new physics in semileptonic operators. This is very different compared to the approach of Ref. [33], which uses short-distance dominated $B \to K^*\mu^+\mu^-$ measurements to determine the non-local correlators, thereby assuming SM values of the $b \to s\mu^+\mu^-$ Wilson coefficients. As a consequence, their SM predictions for the angular observables are model-dependent posterior predictions. The study presented here does not suffer from this model dependence, and thus we determine the non-local correlators and provide a *genuine SM prediction* of the angular observables.

The gray band in Fig. 1 shows the result of this "prior" fit for the case of the real part of $\mathcal{H}_\perp(q^2)$. Similar plots for the other correlators are provided in the appendix for completeness.

With these results at hand, we can compute SM predictions for all observables of interest within the range $0 \le q^2 \lesssim 14\,\mathrm{GeV}^2$. One of them is the angular observable P_5' [34], which is the visible face of the "$B \to K^*\mu^+\mu^-$ anomaly" [35]. Our SM prediction for P_5' is represented by the gray band in Fig. 2. We find relatively small uncertainties and a clearly apparent tension with LHCb data (represented by purple boxes in Fig. 2).

Another interesting SM prediction that we obtain from our analysis is:

$$BR(B^0 \to K^{*0}\gamma) = (4.2^{+1.7}_{-1.3}) \cdot 10^{-5}\,, \tag{11}$$

in agreement with the world average [36]. The larger uncertainties as compared to Ref. [37] are due to our doubling of the form factor uncertainties. SM predictions for all other observables will be given elsewhere.

6 New physics analysis

We now perform a fit to $B \to K^*\mu^+\mu^-$ data using as prior information the SM predictions derived in Sect. 5. We include the branching ratio and the angular observables S_i [38] within the q^2 bins in the region $1 \le q^2 \lesssim 14\,\mathrm{GeV}^2$. We use the latest LHCb measurements [39,40], and perform different separate fits, using the results from the maximum-likelihood fit excluding (LLH) and including (LLH2) the inter-resonance bin, or using the results from the method of moments [41] (MOM and MOM2), and both including (NP fit) and not including (SM fit) a floating NP contribution to C_9.

The fits provide posterior distributions for the correlator, for $B \to K^*\mu^+\mu^-$ and $B \to K^*\gamma$ observables, and for C_9. We first discuss some illustrative results of the LLH2 fit. The posteriors for the real part of $\mathcal{H}_\perp(q^2)$ are shown in Fig. 1, both for the SM and the NP fits. In this case it is reassuring that both are consistent within errors with the result of the prior fit, indicating that modifying the long-distance contribution does not lead to improvement in the SM fit, and so the long-distance contribution is not likely to mimic a NP contribution.

The posterior NP prediction for P_5' (corresponding to the LLH2 fit) is shown in Fig. 2, exhibiting a much better

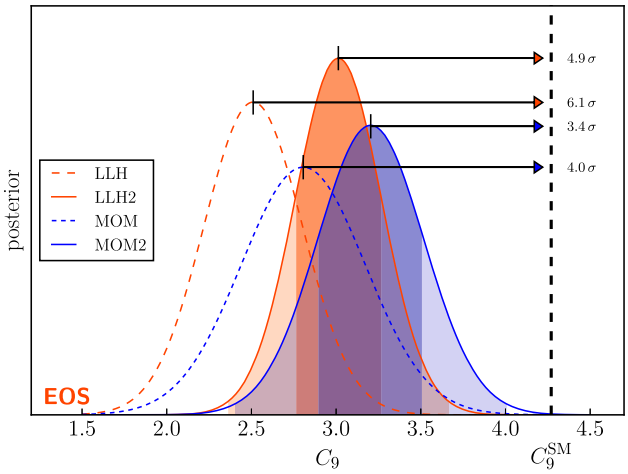

Fig. 3 Posterior distributions for C_9 from the NP fits and their respective pulls. Dark and light shaded regions correspond to 68% and 99% probability

agreement with the experimental measurements than the SM (prior) prediction.

The main conclusion of the fits is the following. The SM fits are relatively inefficient in comparison with the NP fits, with posterior odds [42] ranging from ~ 2.7 to ~ 10 (on the log scale) in favor of the NP hypothesis. The one-dimensional marginalized posteriors yield:

$$\text{(LLH)} : C_9 = 2.51 \pm 0.29, \tag{12}$$

$$\text{(LLH2)} : C_9 = 3.01 \pm 0.25, \tag{13}$$

$$\text{(MOM)} : C_9 = 2.81 \pm 0.37, \tag{14}$$

$$\text{(MOM2)} : C_9 = 3.20 \pm 0.31. \tag{15}$$

The corresponding pulls with respect to the SM point $C_9^{\rm SM}(\mu = 4.2\ \text{GeV}) = 4.27$ range from 3.4 to 6.1 standard deviations, and are illustrated in Fig. 3. These results, from a fit to $B \to K^*\mu^+\mu^-$ data only, are in qualitative agreement with *global* fits [42–48], but rely on a more fundamented theory treatment.

7 Conclusions

Analyticity provides strong constraints on the hadronic contribution to $B \to K^*\ell\ell$ observables, and fixes the q^2 dependence up to a polynomial, which under some circumstances is an expansion in a small kinematical parameter. In this letter we have exploited this idea to propose a systematic approach to determine the dominant non-local contributions, which at this time are the main source of theory uncertainty. This approach is systematically improvable with more precise data on $B \to K^*\psi_n$ and/or more precise theory calculations at negative q^2. In addition, this approach allows access to the inter-resonance region, which provides valuable information on short-distance physics. We have focused on $B \to K^*\ell\ell$, but the approach applies to any other $B \to M\ell\ell$ modes such as $B \to \{K, \pi, \rho\}\ell\ell$ and $B_s \to \phi\ell\ell$.

We have performed a numerical analysis implementing this idea, and conclude that significantly improved theory predictions can be obtained, leading to a more precise and robust interpretation of experimental data and an improved sensitivity to short-distance physics. We identify two issues worth exploring further. One has to do with neglecting the OZI-suppressed cut and charmonium width. A dispersive approach should be able to exploit present and future data on charmless non-leptonic multi-body $B \to K^*X$ decays in order to properly bound these presumably small effects. The other has to do with the convergence of the z expansion. In this respect, the fit including $B \to K^*\ell\ell$ data can provide enough constraints to increase the order of the expansion considerably, especially in view of the extraordinary experimental prospects for the next ten years [49]. We thus believe that this approach will become very useful in future analyses of exclusive $b \to s$ and $b \to d$ transitions.

Acknowledgements We thank Wolfgang Altmannshofer, Kirill Chilikin, Gilberto Colangelo, William Detmold, Christoph Hanhart, Robert Jaffe, Alexander Khodjamirian, Bastian Kubis, Thomas Mannel, Joaquim Matias, Mikolaj Misiak, Federico Mescia, Jacobo Ruiz de Elvira, Iain Stewart, David Straub, Lewis Tunstall, Yuming Wang and Roman Zwicky for useful interactions and discussions. CB is supported in part by the DFG SFB/TR 110 "Symmetries and the Emergence of Structure in QCD". CB and DvD acknowledge support from the Munich Institute for Astro- and Particle Physics (MIAPP) of the DFG cluster of excellence "Origin and Structure of the Universe". MC is grateful for support of the Polish National Science Center under the Sonata grant: UMO-2015/17/D/ST2/03532. DvD is supported in part by the Swiss National Science Foundation (SNF) under contract 200021-159720. JV acknowledges funding from the Swiss National Science Foundation, from Explora project FPA2014-61478-EXP, and from the European Union's Horizon 2020 research and innovation programme under the Marie Sklodowska-Curie grant agreement No 700525 'NIOBE'. This research was supported in part by PL-Grid Infrastructure.

Funded by SCOAP[3].

Appendix A: Supplemental details and results

The effective Lagrangian that governs $b \to s$ transitions contains the following terms relevant for our analysis:

$$\mathcal{L}_{\rm eff} = \frac{4G_F}{\sqrt{2}} V_{tb} V_{ts}^* \sum_{i=1,2,7,9,10} C_i(\mu)\, \mathcal{O}_i(\mu) + \cdots \tag{A1}$$

with the current-current operators defined as

$$\mathcal{O}_1 = \left[\bar{s}\gamma^\mu P_L T^A c\right]\left[\bar{c}\gamma_\mu P_L T^A b\right], \tag{A2}$$

$$\mathcal{O}_2 = \left[\bar{s}\gamma^\mu P_L c\right]\left[\bar{c}\gamma_\mu P_L b\right], \tag{A3}$$

such that $C_2(\mu = M_W) = 1 + \mathcal{O}(\alpha_s)$, with $P_{L(R)} = (1 \mp \gamma_5)/2$ and T^A the generators of SU(3), and the dipole and semileptonic operators given by

$$\mathcal{O}_7 = \frac{e\, m_b}{(4\pi)^2}\left[\bar{s}\sigma^{\mu\nu} P_R b\right] F_{\mu\nu}, \tag{A4}$$

$$\mathcal{O}_9 = \frac{\alpha_e}{4\pi}\left[\bar{s}\gamma^\mu P_L b\right]\left[\bar{\ell}\gamma_\mu \ell\right], \tag{A5}$$

$$\mathcal{O}_{10} = \frac{\alpha_e}{4\pi}\left[\bar{s}\gamma^\mu P_L b\right]\left[\bar{\ell}\gamma_\mu\gamma_5 \ell\right]. \tag{A6}$$

In the SM, the values of the Wilson coefficients are:

$$\begin{aligned} &C_1^{\rm SM}(m_b) = -0.3, \quad C_2^{\rm SM}(m_b) = 1.0, \\ &C_7^{\rm SM}(m_b) = -0.3, \\ &C_9^{\rm SM}(m_b) = 4.3, \qquad C_{10}^{\rm SM}(m_b) = -4.2\,. \end{aligned} \tag{A7}$$

The Lorentz decomposition for the form factors that we use in this analysis is given by

$$\begin{aligned} \langle\bar{s}\gamma^\mu b\rangle &= \eta_\alpha^*\, S_\perp^{\alpha\mu}\mathcal{F}_\perp\,, \\ \langle\bar{s}\gamma^\mu\gamma_5 b\rangle &= \eta_\alpha^*\,(S_\parallel^{\alpha\mu}\mathcal{F}_\parallel + S_0^{\alpha\mu}\mathcal{F}_0 + S_t^{\alpha\mu}\mathcal{F}_t)\,, \\ \langle\bar{s}\sigma^{\mu\nu}q_\nu b\rangle &= i M_B\, \eta_\alpha^*\, S_\perp^{\alpha\mu}\mathcal{F}_\perp^T\,, \\ \langle\bar{s}\sigma^{\mu\nu}q_\nu\gamma_5 b\rangle &= -i M_B\, \eta_\alpha^*\big(S_\parallel^{\alpha\mu}\mathcal{F}_\parallel^T + S_0^{\alpha\mu}\mathcal{F}_0^T\big)\,, \end{aligned} \tag{A8}$$

denoting $\langle\Gamma\rangle \equiv \langle\bar{K}^*(k,\eta)|\Gamma|\bar{B}(q+k)\rangle$. The non-local correlator $\mathcal{H}^{\alpha\mu}$ is decomposed analogously according to Eq. (4):

$$\mathcal{H}^{\alpha\mu} = M_B^2\left[S_\perp^{\alpha\mu}\,\mathcal{H}_\perp - S_\parallel^{\alpha\mu}\,\mathcal{H}_\parallel - S_0^{\alpha\mu}\,\mathcal{H}_0\right].$$

The Lorentz structures $S_\lambda^{\alpha\mu}$ are given by:

$$\begin{aligned} S_\perp^{\alpha\mu} &= \frac{\sqrt{2}M_B}{\sqrt{\lambda(q^2)}}\varepsilon^{\alpha\mu\rho\sigma}k_\rho q_\sigma\,, \\ S_\parallel^{\alpha\mu} &= \frac{i M_B}{\sqrt{2}\lambda(q^2)}\Big[\lambda(q^2)g^{\alpha\mu} + 4M_{K^*}^2 q^\alpha q^\mu - 4(q\cdot k)\,q^\alpha k^\mu\Big]\,, \\ S_0^{\alpha\mu} &= -\frac{i\,4M_{K^*}(M_B + M_{K^*})}{\lambda(q^2)\sqrt{q^2}}\Big[(q\cdot k)\,q^\alpha q^\mu - q^2\,q^\alpha k^\mu\Big]\,, \\ S_t^{\alpha\mu} &= \frac{i\,2M_{K^*}}{q^2}q^\alpha q^\mu\,, \end{aligned} \tag{A9}$$

where the kinematic function $\lambda(q^2)$ is defined as

$$\lambda(q^2) = \left[(M_B + M_{K^*})^2 - q^2\right]\left[(M_B - M_{K^*})^2 - q^2\right]. \tag{A10}$$

Table 2 Uncorrelated priors for the CKM parameters in our analysis, taken from the tree-level-only fit in Ref. [50]

Parameter	Prior (68% gaussian)
λ	0.225 ± 0.006
A	0.829 ± 0.012
$\bar{\rho}$	0.132 ± 0.018
$\bar{\eta}$	0.348 ± 0.012

Table 3 Pseudo-observables from $B \to K^*\psi_n$

Pseudo-observable	Value (68% gaussian)
$\lvert r_\perp^{J/\psi}\rvert$	$(2.027 \pm 0.190)\cdot 10^{-3}$
$\lvert r_\parallel^{J/\psi}\rvert$	$(1.713 \pm 0.260)\cdot 10^{-3}$
$\lvert r_0^{J/\psi}\rvert$	$(2.303 \pm 0.357)\cdot 10^{-3}$
$\arg\{r_\perp^{J/\psi} r_0^{J/\psi *}\}$	$+2.926 \pm 0.032$
$\arg\{r_\parallel^{J/\psi} r_0^{J/\psi *}\}$	-2.944 ± 0.036
$\lvert r_\perp^{\psi(2S)}\rvert$	$(1.06 \pm 0.21)\cdot 10^{-3}$
$\lvert r_\parallel^{\psi(2S)}\rvert$	$(0.98 \pm 0.18)\cdot 10^{-3}$
$\lvert r_0^{\psi(2S)}\rvert$	$(1.40 \pm 0.36)\cdot 10^{-3}$
$\arg\{r_\perp^{\psi(2S)} r_0^{\psi(2S)*}\}$	$+2.799 \pm 0.314$
$\arg\{r_\parallel^{\psi(2S)} r_0^{\psi(2S)*}\}$	-2.815 ± 0.403

The experimental constraints in Sect. 3 are based on the experimental pseudo-observables in Eq. (9), which are obtained by fit to $B \to K^*\psi_n$ data. For $B \to K^* J/\psi$ this data includes the branching ratio as measured by Belle [30], as well as the full set of angular observables $F_\perp$, $F_\parallel$, $\delta_\perp$ and $\delta_\parallel$ measured by BaBar [27] and LHCb [31]. For $B \to K^*\psi(2S)$ the data includes the branching ratio and the longitudinal polarization measured by Belle [29], and the full set of angular observables from BaBar [27]. For all measurements, correlations have been taken into account where available. More recent results for the full angular distributions, stemming from amplitude analyses that take into account tetra-quark contributions [29,30], are not used here. The ansatz involving tetra-quark amplitudes is incompatible with the basis of our analysis. Although we expect to be able to use these additional results in future studies, this requires further dedicated work.

The relevant input to this fit are the CKM parameters, listed in Table 2, and the form factors (see Eq. (10)). Since the experimental inputs are sensitive to the form factors at $q^2 \leq 10\ \text{GeV}^2$, we use the combined fit to K^*-meson LCSR and Lattice results performed in Ref. [6]. However, we *double* the uncertainties quoted in [6] to ensure full agreement among the LCSRs and Lattice results. Note that we do not account for correlations among the $r_\lambda^{\psi_n}$ due to correlations among the form factor parameters. The results for the pseudo-

Table 4 Mean values μ_i (in units of 10^{-4}), and standard deviations σ_i (in units of 10^{-4}) of the theory constraints at negative q^2 (in units of GeV^2)

	$\mathrm{Re}[\mathcal{H}_\perp]/\mathcal{F}_\perp$				$\mathrm{Re}[\mathcal{H}_\parallel]/\mathcal{F}_\parallel$				$\mathrm{Re}[\mathcal{H}_0]/\mathcal{F}_0$			
q^2	− 7.0	− 5.0	− 3.0	− 1.0	− 7.0	− 5.0	− 3.0	− 1.0	− 7.0	− 5.0	− 3.0	− 1.0
μ	6.656	4.878	4.076	3.750	6.033	4.384	3.728	3.586	− 1.997	1.596	1.818	0.768
σ	2.553	1.048	0.621	0.561	2.446	0.971	0.575	0.538	4.077	1.368	0.472	0.125
	$\mathrm{Im}[\mathcal{H}_\perp]/\mathcal{F}_\perp$				$\mathrm{Im}[\mathcal{H}_\parallel]/\mathcal{F}_\parallel$				$\mathrm{Im}[\mathcal{H}_0]/\mathcal{F}_0$			
q^2	−7.0	−5.0	−3.0	−1.0	−7.0	−5.0	−3.0	−1.0	−7.0	−5.0	−3.0	−1.0
μ	1.581	1.294	1.291	1.380	1.517	1.246	1.257	1.366	6.328	1.970	0.583	0.136
σ	0.835	0.610	0.565	0.585	0.803	0.590	0.553	0.581	7.411	2.107	0.528	0.082

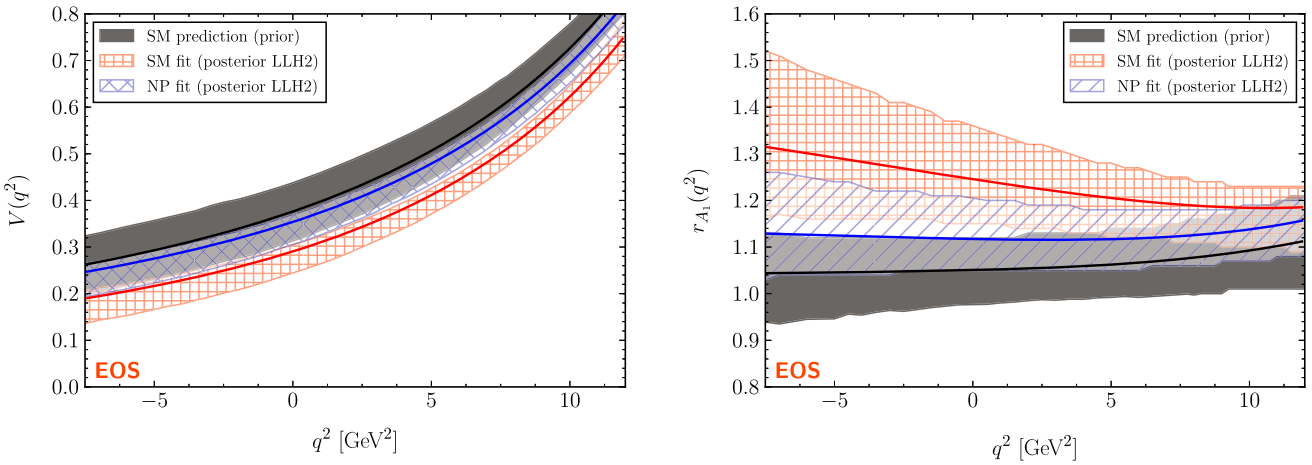

Fig. 4 A-priori predictions of the form factor V and the symmetry ratio r_{A_1} as functions of q^2, and comparison with two a-posteriori results

observables are given in Table 3. The two sets of observables for J/ψ and $\psi(2S)$ are correlated with correlation matrices:

$$\rho_{J/\psi} = \begin{pmatrix} 1.000 & 0.786 & 0.213 & -0.007 & -0.026 \\ & 1.000 & 0.177 & 0.003 & 0.011 \\ & & 1.000 & -0.003 & -0.004 \\ & & & 1.000 & 0.652 \\ & & & & 1.000 \end{pmatrix}, \tag{A11}$$

$$\rho_{\psi(2S)} = \begin{pmatrix} 1.000 & -0.116 & 0.233 & -0.222 & -0.204 \\ & 1.000 & 0.252 & 0.204 & 0.173 \\ & & 1.000 & -0.007 & 0.008 \\ & & & 1.000 & 0.679 \\ & & & & 1.000 \end{pmatrix}. \tag{A12}$$

In both cases, the mean and standard deviations have been obtained from a fit to 10^6 samples of the posterior predictive distributions. On the other hand, the correlation coefficients have been obtained from the sample covariance of these 10^6 samples. It is noteworthy that none of the coefficients exceeds a level of 78% for the J/ψ and 68% for the $\psi(2S)$, respectively.

The theory constraints in Sect. 4 are based on pseudo-observables at four different points at spacelike q^2. The derived values including uncertainties and correlations are listed in Table 4.

Nominally, for $K = 2$ the fit would involve 18 real-valued parameters $\alpha_k^{(\lambda)}$. Using the property that the longitudinal correlator must vanish at zero momentum transfer $q^2 = 0$, $\hat{\mathcal{H}}_0(z(q^2 = 0)) = 0$, we can reduce the number of parameters by 2 through the replacement

$$\begin{aligned} \alpha_0^{(0)} &\to \alpha_0'^{(0)} \equiv -z(0)\,\alpha_0^{(0)}\,, \\ \alpha_1^{(0)} &\to \alpha_1'^{(0)} \equiv \alpha_0^{(0)} - z(0)\,\alpha_1^{(0)}\,, \\ \alpha_2^{(0)} &\to \alpha_2'^{(0)} \equiv \alpha_1^{(0)}\,. \end{aligned} \tag{A13}$$

From the fit of the parameters $\alpha_k^{(\lambda)}$ to the theory constraints and the pseudo-observables $r_\lambda^{\psi_n}$ we find all 1D-marginalized posteriors to be reasonably symmetric around their modes. As for the pseudo-observables, we obtain means and standard deviations from fits to 10^6 samples of the PDF, while the correlation coefficients are obtained through computation of the sample covariance. Our results are summarized in Table 1. Finally, the set of predictive distributions for the ratios $\mathcal{H}_\lambda/\mathcal{F}_\lambda$ are shown in Fig. 5 for all transversities, including real and imaginary parts.

A key result of our analysis is that modifications to the correlator parameters cannot bring the theory predictions

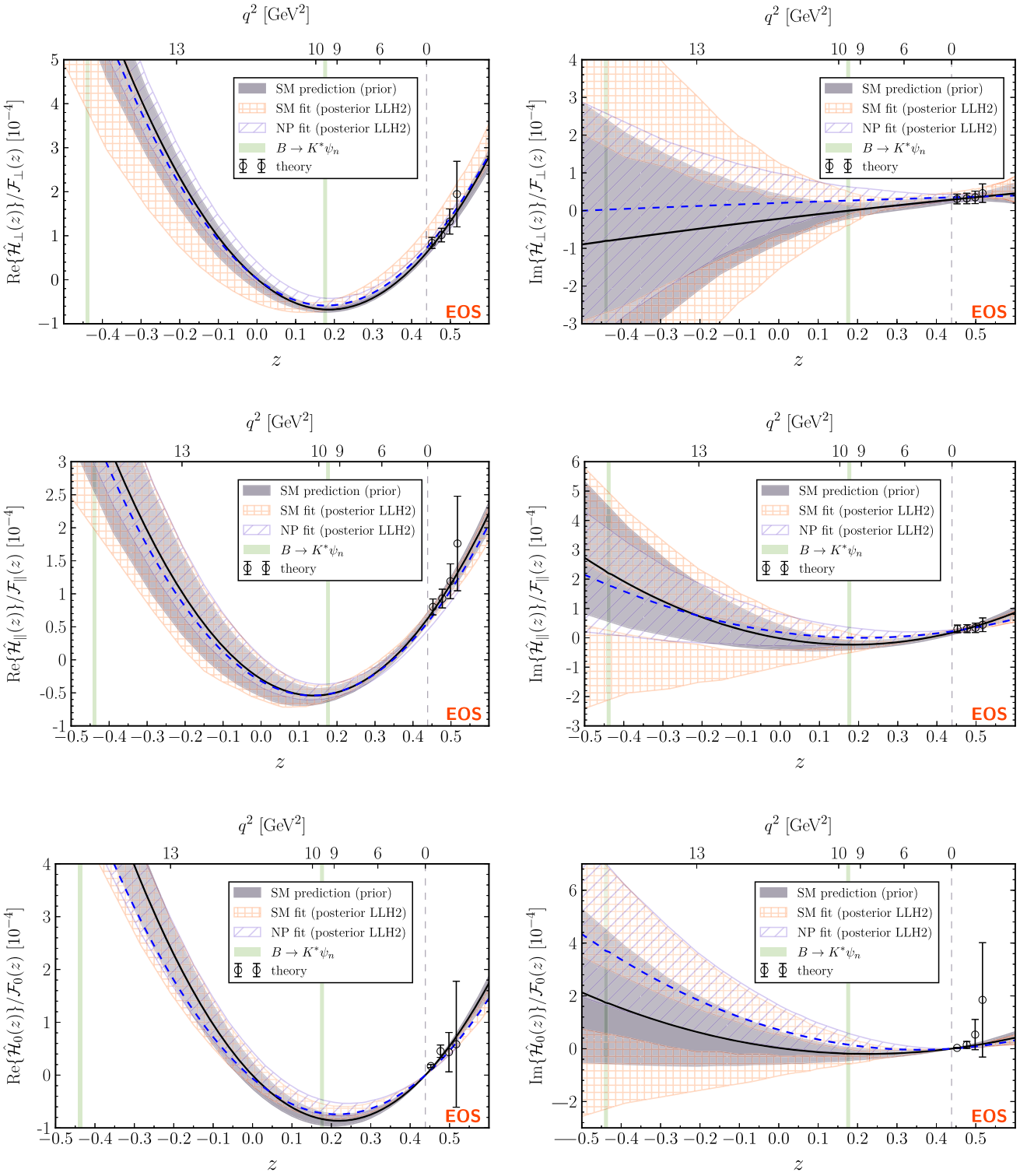

Fig. 5 A-priori predictions of the ratios $\mathcal{H}_\lambda/\mathcal{F}_\lambda$ as functions of z, and comparison with two a-posteriori results. Note that the SM fit posterior is multi-modal, and we therefore choose not to illustrate its best-fit curves

and measurements into better agreement. However, modifications to the form factor parameters can reduce the tensions, albeit not completely. We show in Fig. 4a the impact on the form factor $V(q^2)$, which is the one most affected. Moreover, since the form factor A_1 is almost unaffected, we find that the SM fit prefers a substantial violation of the large-recoil symmetry relation [51,52] involving V and A_1,

$$r_{A_1}(q^2) \equiv \frac{(M_B + M_{K^*})^2}{2M_B E_{K^*}(q^2)} \frac{A_1(q^2)}{V(q^2)}, \tag{A14}$$

as shown in Fig. 4(b).

References

1. P. Ball, V.M. Braun, Exclusive semileptonic and rare B meson decays in QCD. Phys. Rev. D **58**, 094016 (1998). arXiv:hep-ph/9805422 [hep-ph]
2. A. Khodjamirian, T. Mannel, N. Offen, Form-factors from light-cone sum rules with B-meson distribution amplitudes. Phys. Rev. D **75**, 054013 (2007). arXiv:hep-ph/0611193 [hep-ph]
3. D. Becirevic, V. Lubicz, F. Mescia, An Estimate of the $B \to K^*\gamma$ form factor. Nucl. Phys. B **769**, 31–43 (2007). arXiv:hep-ph/0611295 [hep-ph]
4. R.R. Horgan, Z. Liu, S. Meinel, M. Wingate, Lattice QCD calculation of form factors describing the rare decays $B \to K^*\ell^+\ell^-$ and $B_s \to \phi\ell^+\ell^-$. Phys. Rev. D **89**, 094501 (2014). arXiv:1310.3722 [hep-lat]
5. S. Descotes-Genon, T. Hurth, J. Matias, J. Virto, Optimizing the basis of $B \to K^*ll$ observables in the full kinematic range. JHEP **05**, 137 (2013a). arXiv:1303.5794 [hep-ph]
6. A. Bharucha, D.M. Straub, R. Zwicky, $B \to V\ell^+\ell^-$ in the Standard Model from light-cone sum rules. JHEP **08**, 098 (2016). arXiv:1503.05534 [hep-ph]
7. M.T. Hansen, S.R. Sharpe, Multiple-channel generalization of Lellouch-Luscher formula. Phys. Rev. D **86**, 016007 (2012). arXiv:1204.0826 [hep-lat]
8. R.A. Briceo, M.T. Hansen, A. Walker-Loud, Multichannel $1 \to 2$ transition amplitudes in a finite volume. Phys. Rev. D **91**, 034501 (2015). arXiv:1406.5965 [hep-lat]
9. S. Cheng, A. Khodjamirian, J. Virto, $B \to \pi\pi$ Form Factors from Light-Cone Sum Rules with B-meson Distribution Amplitudes. JHEP **05**, 157 (2017). arXiv:1701.01633 [hep-ph]
10. P. Böer, T. Feldmann, D. van Dyk, QCD factorization for $B \to \pi\pi\ell\nu$ decays at large dipion masses. JHEP **02**, 133 (2017). arXiv:1608.07127 [hep-ph]
11. Y.-M. Wang, Y.-L. Shen, QCD corrections to $B \to \pi$ form factors from light-cone sum rules. Nucl. Phys. B **898**, 563–604 (2015). arXiv:1506.00667 [hep-ph]
12. M. Beneke, T. Feldmann, D. Seidel, Systematic approach to exclusive $B \to V\ell^+\ell^-$, $V\gamma$ decays. Nucl. Phys. B **612**, 25–58 (2001). arXiv:hep-ph/0106067 [hep-ph]
13. A. Khodjamirian, T. Mannel, A.A. Pivovarov, Y.M. Wang, Charm-loop effect in $B \to K^{(*)}\ell^+\ell^-$ and $B \to K^*\gamma$. JHEP **09**, 089 (2010). arXiv:1006.4945 [hep-ph]
14. H.H. Asatryan, H.M. Asatrian, C. Greub, M. Walker, Calculation of two loop virtual corrections to $b \to s\ell^+\ell^-$ in the standard model. Phys. Rev. D **65**, 074004 (2002). arXiv:hep-ph/0109140 [hep-ph]
15. A. Khodjamirian, T. Mannel, Y.M. Wang, $B \to K\ell^+\ell^-$ decay at large hadronic recoil. JHEP **02**, 010 (2013). arXiv:1211.0234 [hep-ph]
16. D. van Dyk et al., EOS—A HEP Program for Flavour Observables (2017)
17. D. van Dyk et al. EOS ("analytic-btokstarll" release) (2017)
18. R.J. Eden, P.V. Landshoff, D.I. Olive, J.C. Polkinghorne, *The analytic S-matrix* (Cambridge Univ. Press, Cambridge, 1966)
19. L. Klein, *Dispersion Relations and the Abstract Approach to Field Theory* (Literary Licensing, LLC, 2012)
20. S. Okubo, Phi meson and unitary symmetry model. Phys. Lett. **5**, 165–168 (1963)
21. G. Zweig, An $SU(3)$ model for strong interaction symmetry and its breaking. Version 2, in *Developments in the quark theory of hadrons, vol. 1. 1964–1978*, ed. by D.B. Lichtenberg, Simon Peter Rosen (1964), pp. 22–101
22. J. Iizuka, Systematics and phenomenology of meson family. Prog. Theor. Phys. Suppl. **37**, 21–34 (1966)
23. C. Glenn, Boyd, Benjamin Grinstein, and Richard F. Lebed, Model independent extraction of $|V_{cb}|$ using dispersion relations. Phys. Lett. B **353**, 306–312 (1995). arXiv:hep-ph/9504235 [hep-ph]
24. C. Bourrely, I. Caprini, L. Lellouch, Model-independent description of $B \to \pi\ell\nu$ decays and a determination of $|V_{ub}|$. Phys. Rev. D **79**, 013008 (2009). [Erratum: Phys. Rev.D82,099902(2010)], arXiv:0807.2722 [hep-ph]
25. S. Weinberg, *The Quantum theory of fields. Vol. 1: Foundations* (Cambridge University Press, Cambridge, 2005)
26. B. Aubert et al., (BaBar), Measurement of branching fractions and charge asymmetries for exclusive B decays to charmonium. Phys. Rev. Lett. **94**, 141801 (2005). arXiv:hep-ex/0412062 [hep-ex]
27. B. Aubert et al., (BaBar), Measurement of decay amplitudes of $B \to J/\psi K^*$, $\psi(2S)K^*$, and $\chi_{c1}K^*$ with an angular analysis. Phys. Rev. D **76**, 031102 (2007). arXiv:0704.0522 [hep-ex]
28. R. Itoh et al. (Belle), Studies of CP violation in $B \to J/\psi K^*$ decays, Phys. Rev. Lett. **95**, 091601 (2005). arXiv:hep-ex/0504030 [hep-ex]
29. K. Chilikin et al., (Belle), Experimental constraints on the spin and parity of the $Z(4430)^+$. Phys. Rev. D **88**, 074026 (2013). arXiv:1306.4894 [hep-ex]
30. K. Chilikin et al., (Belle), Observation of a new charged charmoniumlike state in $\bar{B}^0 \to J/\psi K^-\pi^+$ decays. Phys. Rev. D **90**, 112009 (2014). arXiv:1408.6457 [hep-ex]
31. R. Aaij et al., (LHCb), Measurement of the polarization amplitudes in $B^0 \to J/\psi K^*(892)^0$ decays. Phys. Rev. D **88**, 052002 (2013a). arXiv:1307.2782 [hep-ex]
32. M. Beneke, T. Feldmann, D. Seidel, Exclusive radiative and electroweak $b \to d$ and $b \to s$ penguin decays at NLO. Eur. Phys. J. C **41**, 173–188 (2005). arXiv:hep-ph/0412400 [hep-ph]
33. M. Ciuchini, M. Fedele, E. Franco, S. Mishima, A. Paul, L. Silvestrini, M. Valli, $B \to K^*\ell^+\ell^-$ decays at large recoil in the Standard Model: a theoretical reappraisal, (2015). arXiv:1512.07157 [hep-ph]
34. S. Descotes-Genon, J. Matias, M. Ramon, J. Virto, Implications from clean observables for the binned analysis of $B \to K^*\mu^+\mu^-$ at large recoil. JHEP **01**, 048 (2013b). arXiv:1207.2753 [hep-ph]
35. R. Aaij et al., (LHCb), Measurement of Form-Factor-Independent Observables in the Decay $B^0 \to K^{*0}\mu^+\mu^-$. Phys. Rev. Lett. **111**, 191801 (2013b). arXiv:1308.1707 [hep-ex]
36. Y. Amhis et al., Averages of b-hadron, c-hadron, and τ-lepton properties as of summer 2016, (2016). arXiv:1612.07233 [hep-ex]
37. A. Paul, D.M. Straub, Constraints on new physics from radiative B decays. JHEP **04**, 027 (2017). arXiv:1608.02556 [hep-ph]
38. W. Altmannshofer, P. Ball, A. Bharucha, A.J. Buras, D.M. Straub, M. Wick, Symmetries and Asymmetries of $B \to K^*\mu^+\mu^-$ Decays in the Standard Model and Beyond. JHEP **01**, 019 (2009). arXiv:0811.1214 [hep-ph]
39. R. Aaij et al., (LHCb), Angular analysis of the $B^0 \to K^{*0}\mu^+\mu^-$ decay using 3 fb^{-1} of integrated luminosity. JHEP **02**, 104 (2016a). arXiv:1512.04442 [hep-ex]

40. R. Aaij et al., (LHCb), Measurements of the S-wave fraction in $B^0 \to K^+\pi^-\mu^+\mu^-$ decays and the $B^0 \to K^*(892)^0\mu^+\mu^-$ differential branching fraction. JHEP **11**, 047 (2016b). arXiv:1606.04731 [hep-ex]
41. F. Beaujean, M. Chrzaszcz, N. Serra, D. van Dyk, Extracting Angular Observables without a Likelihood and Applications to Rare Decays. Phys. Rev. D **91**, 114012 (2015). arXiv:1503.04100 [hep-ex]
42. F. Beaujean, C. Bobeth, D. van Dyk, Comprehensive Bayesian analysis of rare (semi)leptonic and radiative B decays. Eur. Phys. J. C **74**, 2897 (2014). [Erratum: Eur. Phys. J.C74,3179(2014)], arXiv:1310.2478 [hep-ph]
43. S. Descotes-Genon, J. Matias, J. Virto, Understanding the $B \to K^*\mu^+\mu^-$ Anomaly. Phys. Rev. D **88**, 074002 (2013c). arXiv:1307.5683 [hep-ph]
44. W. Altmannshofer, D.M. Straub, New Physics in $B \to K^*\mu\mu$? Eur. Phys. J. C **73**, 2646 (2013). arXiv:1308.1501 [hep-ph]
45. W. Altmannshofer, C. Niehoff, P. Stangl, D.M. Straub, Status of the $B \to K^*\mu^+\mu^-$ anomaly after Moriond 2017. Eur. Phys. J. C **77**, 377 (2017). arXiv:1703.09189 [hep-ph]
46. B. Capdevila, A. Crivellin, Sébastien Descotes-Genon, Joaquim Matias, Javier Virto, Patterns of New Physics in $b \to s\ell^+\ell^-$ transitions in the light of recent data. JHEP **1801**, 093 (2018). arXiv:1704.05340 [hep-ph]
47. L.S. Geng, B. Grinstein, S. Jäger, J. Martin Camalich, X.L. Ren, R.X. Shi, Towards the discovery of new physics with lepton-universality ratios of $b \to s\ell\ell$ decays. Phys. Rev. D **96**, 093006 (2017). arXiv:1704.05446 [hep-ph]
48. T. Hurth, F. Mahmoudi, D. Martinez Santos, S. Neshatpour, On lepton non-universality in exclusive $b \to s\ell\ell$ decays. Phys. Rev. D **96**, 095034 (2017). arXiv:1705.06274 [hep-ph]
49. M. Chrzaszcz, A. Mauri, N. Serra, R. Silva Coutinho, D. van Dyk, Prospects for data-driven analyses of the decays $b \to k^*\ell^+\ell^-$, (TUM-HEP-1108/17, ZU-TH 25/17). arXiv:1805.06378 [hep-ph]
50. M. Bona et al., (UTfit Collaboration), The Unitarity Triangle Fit in the Standard Model and Hadronic Parameters from Lattice QCD: A Reappraisal after the Measurements of Δm_s and BR($B \to \tau\nu_\tau$). JHEP **0610**, 081 (2006). we use the updated data from Winter 2013 (pre-Moriond 13). arXiv:hep-ph/0606167 [hep-ph]
51. J. Charles, A. Le Yaouanc, L. Oliver, O. Pene, J.C. Raynal, Heavy to light form-factors in the heavy mass to large energy limit of QCD. Phys. Rev. D **60**, 014001 (1999). arXiv:hep-ph/9812358 [hep-ph]
52. M. Beneke, T. Feldmann, Symmetry breaking corrections to heavy to light B meson form-factors at large recoil. Nucl. Phys. B **592**, 3–34 (2001). arXiv:hep-ph/0008255 [hep-ph]